Journal of Instrumentation

PAPER • **OPEN ACCESS**

Characterization of scintillator screens under irradiation of low energy ^{133}Cs ions

To cite this article: J.J. Toledo-Garrido *et al* 2022 *JINST* **17** P02026

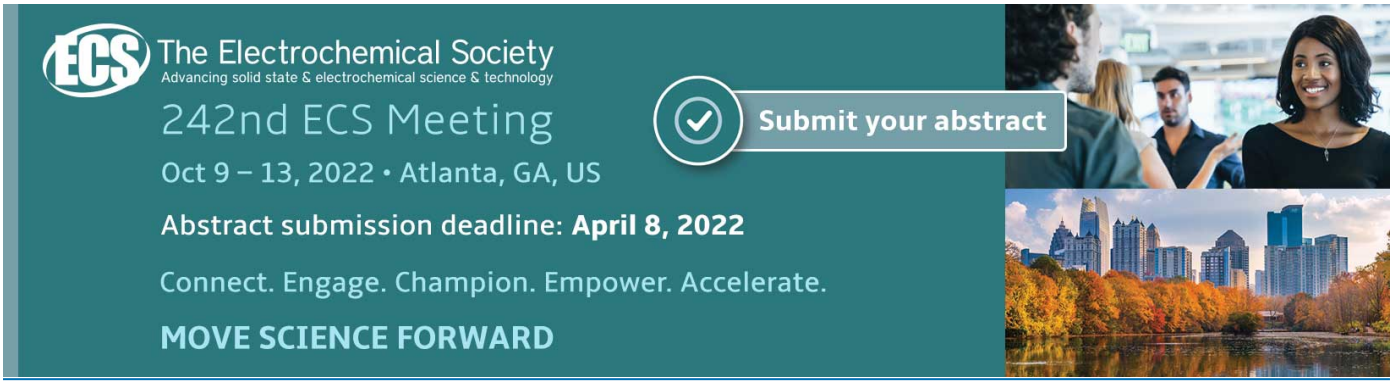

Published by IOP Publishing for Sissa Medialab

Received: *December 25, 2021*
Revised: *January 26, 2022*
Accepted: *January 30, 2022*
Published: *February 18, 2022*

Characterization of scintillator screens under irradiation of low energy ^{133}Cs ions

J.J. Toledo-Garrido,[a,b] **J. Galdon-Quiroga,**[a,c,*] **E. Viezzer,**[a,b] **G. Birkenmeier,**[c,d] **V. Olevskaia,**[d] **M. Balden,**[c] **J. Garcia-Lopez,**[a,b] **M.C. Jimenez-Ramos,**[a,b] **M. Rodriguez-Ramos,**[e] **G. Anda,**[f] **M. Videla-Trevin,**[b] **M. Garcia-Munoz**[a,b] **and the ASDEX Upgrade Team**

[a] *Departamento de Física Atómica, Molecular y Nuclear, Universidad de Sevilla, Facultad de Física, Avda. Reina Mercedes s/n 41012, Seville, Spain*
[b] *Centro Nacional de Aceleradores (Universidad de Sevilla, Junta de Andalucia, CSIC), C/ Thomas Alva Edison 7, 41092, Seville, Spain*
[c] *Max Planck Institute for Plasma Physics, Boltzmannstrasse 2, 85748, Garching bei Muenchen, Germany*
[d] *Physics Department E28, Technical University of Munich, James-Franck-Str. 1, 85748, Garching bei Muenchen, Germany*
[e] *Laboratory for Ion Beam Interaction, Ruder Boskovic Institute, Bijenicka cesta 54, Zagreb, Croatia*
[f] *Fusion Technology Department, Centre for Energy Research, Konkoly-Thege Miklós út, 1121, Budapest, Hungary*

E-mail: jgaldon@us.es

Abstract: An imaging heavy ion beam probe (i-HIBP) diagnostic, for the simultaneous measurement of plasma density, magnetic field and electrostatic potential in the plasma edge, has been installed at ASDEX Upgrade. Unlike standard heavy ion beam probes, in the i-HIBP the probing (heavy) ions are collected by a scintillator detector, creating a light pattern or strike-line, which is then imaged by a camera. Therefore, a good characterization of the scintillator response is needed. Previous works focused on the scintillator behaviour against irradiation with light ions such as hydrogen and alpha particles. In this work we present the characterization of several scintillator screens — TG-Green ($SrGa_2S_4$:Eu_2^+), YAG-Ce ($Y_3Al_5O_{12}$:Ce_3^+) and P11 (ZnS:Ag) — against irradiation with $^{133}Cs^+$ ions, in an energy range between 5 and 70 keV and ion currents between 10^5 and 10^7 ions/(s·cm^2). Three main properties of the scintillators have been studied: the ionolumenescence efficiency or yield, the linearity and the degradation as a function of the fluence. The highest yield was delivered by the TG-Green scintillator screen with $> 8 \cdot 10^3$ photons/ion at 50 keV. All the samples showed a linear response with increasing incident ion flux. The degradation was quantified in terms of the fluence

*Corresponding author.

https://doi.org/10.1088/1748-0221/17/02/P02026

$F_{1/2}$, which leads to a reduction of the emissivity by a factor of 2. TG-Green showed the lowest degradation with $F_{1/2} = 5.4 \cdot 10^{14}$ ions/cm^2. After the irradiation the samples were analyzed by Scanning Electron Microscopy (SEM), Rutherford Backscattering Spectrometry (RBS) and Particle Induced X-ray Emission (PIXE). No trace of Cs was found in the irradiated regions. These results indicate that, among the tested materials, TG-Green is the best candidate for the i-HIBP detector.

KEYWORDS: Scintillators, scintillation and light emission processes (solid, gas and liquid scintillators); Heavy-ion detectors; Plasma diagnostics - probes

2022 JINST 17 P02026

Contents

1 Introduction **1**

2 Scintillator screens **2**
- 2.1 Description of scintillators 2
- 2.2 Scintillator coating by sedimentation process at CNA 2

3 Experimental set-up **3**

4 Results **4**
- 4.1 Ionoluminiscence degradation of the scintillators 4
- 4.2 Calibrated photon detection yield of scintillators as a function of incident ion energy 5
- 4.3 Linearity of ionoluminiscence with ion current 7
- 4.4 Composition and thickness of the scintillators 8

5 Summary and conclusions **9**

1 Introduction

A new diagnostic, the Imaging Heavy Ion Beam Probe (i-HIBP), has been installed in the ASDEX Upgrade (AUG) tokamak at the Max Planck Institute for Plasma Physics (IPP) [1–3]. Unlike standard heavy ion beam probes, in the i-HIBP the probing (heavy) ions are collected by a scintillator detector, creating a light pattern or strike-line, which is then imaged by a camera. Information about the magnetic field and electrostatic potential fluctuations can be retrieved from the strike-line shape and displacement. The plasma density profile can be retrieved from the signal intensity, for which a comprehensive knowledge of the scintillator response is needed. A more detailed description of the measurement principle of the i-HIBP can be found in [1, 3].

Ionoluminescence consists in the emission of light by a material when it is irradiated by ions. This process could be described as the de-excitation of stimulated electronic states, related either to valence electrons of particular atoms or to defects inside crystalline structures [4]. Previous work focused on the study of the ionoluminescence of several scintillators when they are irradiated by light ions, for its application in Fast Ion Loss Detectors (FILD) [5, 6]. In this work we focus on the study of scintillator response to irradiation with heavy ions. In particular, we will use ^{133}Cs which corresponds to the species of the primary beam selected for the i-HIBP at AUG. In this study we have characterized the ionoluminescence of four scintillators screens; two TG-Green plates ($SrGa_2S_4$:Eu_2^+) (one provided by Sarnoff Corporation and another coated at Centro Nacional de Aceleradores (CNA)), YAGCe ($Y_3Al_5O_{12}$:Ce_3^+) and P11 (ZnS:Ag), to estimate which one is the most appropriate for the diagnostic. The ionoluminescence of these materials should meet the following requirements:

2022 JINST 17 P02026

- A high efficiency or yield, i.e. number of emitted photons per irradiated ion (expected current densities at the i-HIBP scintillator plate of mA/m^2 [1]). A high yield means a high i-HIBP signal.
- A linear behaviour of the emission with incident current is needed for signal interpretation.
- Low scintillator degradation: ions create defects in the structure of the material that degrade the ionoluminescence, i.e. inhibit light emission. This characterization is related with the i-HIBP signal intensity and the "life-time" of the scintillator.

In section 2 the composition and emission of the scintillators is described. Besides, the sedimentation process, for which TG-Green-A screen was coated, is detailed. Section 3 deals with a brief description of the experimental set up. In section 4 the results of the measurements of ionoluminescence efficiency, degradation and linearity with incident current of the scintillators are discussed. Furthermore, a composition and thickness analysis of the materials was set. Finally, section 5 summarizes and concludes this investigation.

2 Scintillator screens

2.1 Description of scintillators

TG-Green is used in ASDEX Upgrade FILD detectors due to its high efficiency and fast response [7, 8]. YAGCe is a solid candidate to be used in i-HIBP diagnostic due to its high efficiency when it is ionized by light particles [7]. P11 has a long decay time of 3 ms, which is unfavorable, but serves as a benchmark material for comparison to the others. In table 1 some information about the scintillators used in this study is collected: its composition, the wavelength range of the emissions and the suppliers of the materials.

Table 1. Scintillator information. a See section 4. b The difference between emissions of TG-Green-A and TG-Green-B could be due to their different compositions (see section 4).

Scintillator	Composition	Provided by	Wavelength Range (nm)	FWHM (nm)
TG-Green-A	—[a]	Coated in CNA	470–720[b]	80
TG-Green-B	$SrGa_2S_4:Eu^{2+}$	Sarnoff Corporation	475–620[b]	45
YAGCe	$Y_3Al_5O_{12}:Ce^{3+}$	CRYTUR	470–730	108
P11	ZnS:Ag	Coated in CNA	380–620	64

In figure 1 the emission spectrum of the different scintillator materials is shown. It can be seen that TG-Green-A and TG-Green-B show some differences in their emission spectrum. It could be explained by the composition of the materials (see section 4.4).

2.2 Scintillator coating by sedimentation process at CNA

One of the TG-Green plates ($4.4 \times 3.3\,cm^2$) and the P11 scintillator was deposited at the Centro Nacional de Aceleradores (Seville) using the sedimentation process [9]. This technique consists in making a solution of the scintillator powder and an adhesive and pouring it over a stainless steel

2022 JINST 17 P02026

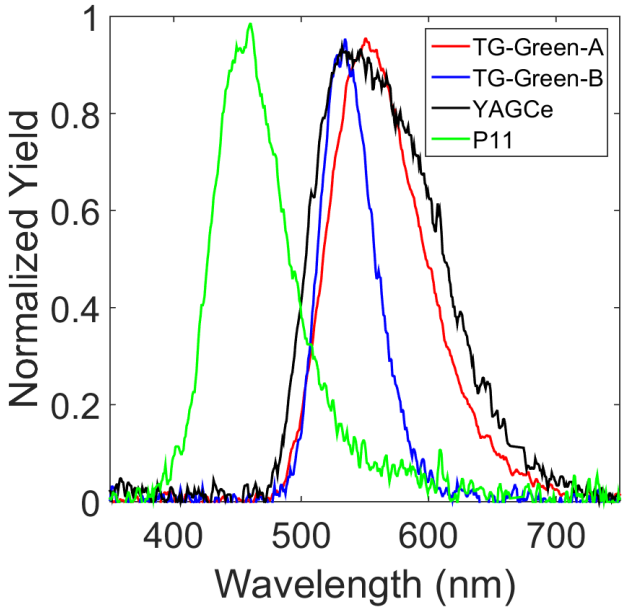

Figure 1. Ionoluminiscence spectrum of the following scintillators irradiated by ^{133}Cs at 50 keV: TG-Green-A (red), TG-Green-B (blue), YAGCe (black) and P11 (magenta).

substrate. We choose the sedimentation process due to its easy approach and the uniformity of the layers, which is achievable with this technique. The sedimentation of the layers was performed using a mixture of 1.5 g of the scintillator powder dispersed in 40 ml of a 0.1% liquid solution of sodium hexametaphosphate ($NaPO_3$) which acts as adhesive. The solution is then mixed at 300 rpm and heated at 60°C during 1 hour. Once the mix is ready, it is poured over the metal substrate. When the solution is cooled down and the powder mix has formed an uniform layer over the substrate, we remove the water using a pipette and dry the metal plates in an oven at 140°C for 10 minutes.

3 Experimental set-up

The characterization of the scintillator response to irradiation with $^{133}Cs^+$ ions was performed using the ASDEX Upgrade i-HIBP beam injector. The injector is based on the design described in [10] and has been provided by the Centre for Energy Research (Budapest, Hungary). The main elements of the injector are a high-voltage cage that contains the ion source, the emitter and extractor electrodes, an electron suppression ring and a pair of deflection plates. These plates allow poloidal and toroidal beam steering as well as fast beam chopping. A collimator with a diameter of 1 mm is placed at the end of the injector to define the beam size and position on the scintillator.

The samples under study were placed in an electrically isolated holder inside a vacuum chamber with a black coating to minimize light reflection with an inclination of 45° in the vertical axis. The vertical movement of the sample holder was controlled manually by a worm drive, perpendicular to the ion beam axis. The light emission was collected by a silica optical fiber of a diameter of 440 µm fixed to a port of the vacuum chamber. This fiber was connected to a high-sensitivity spectrometer (QE65000, Ocean Optics Inc. Quantum Efficiency of 90% peak) which allows making

2022 JINST 17 P02026

simultaneous measurements in the range of 199.05–1000.04 nm with a spectral resolution of 1–2 nm. The measured signals were analyzed and stored with the SpectraSuite software [11]. The calibration of the optical system has been done with a HL-2000-CAL tungsten halogen standard calibration light source. This calibration gives the spectrometer software the relation between the energy measured by the CCD camera and the number of photons emitted by the tungsten light source. On the other hand, the spectrometer takes the data for a certain amount of time (given by the user), so by integrating the calibrated spectra of the spectrometer one could obtain the total amount of photons that was measured during the time set by the user (photons/s). In order to get the total amount of photons emitted by the scintillators (and not only the one collected by the optical fiber) a solid angle correction was applied. This method was done with the same spectrometer and calibration light source as in [8].

The incident ion current was measured by a Faraday cup which is within a secondary electron suppression ring and is placed behind the sample holder. Due to the position of the Faraday Cup, simultaneous measurement of the incident current and the scintillator emission was not possible. Instead, the ion current was measured in a first shot with the sample holder in a low position. Then, the sample holder was brought into position and a second shot was performed in which the scintillator was irradiated, thus producing the light emission.

4 Results

4.1 Ionoluminiscence degradation of the scintillators

The ionoluminescence of a scintillator suffers degradation with accumulated ion fluence. To investigate this effect, we carried out a sequence of shots with a duration of $\sim$ 10 s at a fixed beam energy of 55 keV and beam currents of $\sim 10^6$ ions/(s·cm^2). During each sequence the exact same point of the scintillator sample was irradiated. Figure 2 shows the degradation of the ionoluminescence emission as a function of incident fluence. The Black-Birk model (eq. (4.1)) [12] describes the degradation of the ionoluminescence of a scintillator when it suffers by ionization with a certain energy.

$$\frac{L_0}{L} - 1 = \frac{F}{F_{1/2}} \tag{4.1}$$

Here, L_0 is the initial emission of the scintillator, L is the emission of the scintillator after a fluence F has damaged it and $F_{1/2}$ is the fluence needed to reduce its emission to 50% of its initial emission. A linear fit between $L_0/L - 1$ and F gives a slope equal to $1/F_{1/2}$ (see figure 2), so we could compare this result with $F_{1/2}$ by reading the fluence value at which each curve crosses the normalized emission value of 0.5 (table 2). TG-Green-A has the slowest degradation and P11 has the fastest degradation of the studied scintillators, all of them showing an $F_{1/2}$ of the order of 10^{14} ions/cm^2 These values can be compared to previous work [13] where a $F_{1/2}$ of $3.7 \cdot 10^{15}$ ions/cm^2, $9.82 \cdot 10^{14}$ ions/cm^2 and $4.36 \cdot 10^{14}$ ions/cm^2, was found for TG-Green when irradiated by light ions (H^+, D^+ and He^{++}) at 1 MeV, and a $F_{1/2}$ of $2.56 \cdot 10^{16}$ ions/cm^2 and $7.3 \cdot 10^{15}$ ions/cm^2 for YAGCe and TG-Green respectively when irradiated by D^+ at 2 MeV.

Different mechanisms can play a role in the degradation of the scintillator light yield when irradiated by ions [14]. Amongst them, the most common mechanism is the radiation induced absorption, which leads to the formation of color centers that effectively attenuate the light output emitted by the scintillation process [15]. Our observations, together with the results reported in

2022 JINST 17 P02026

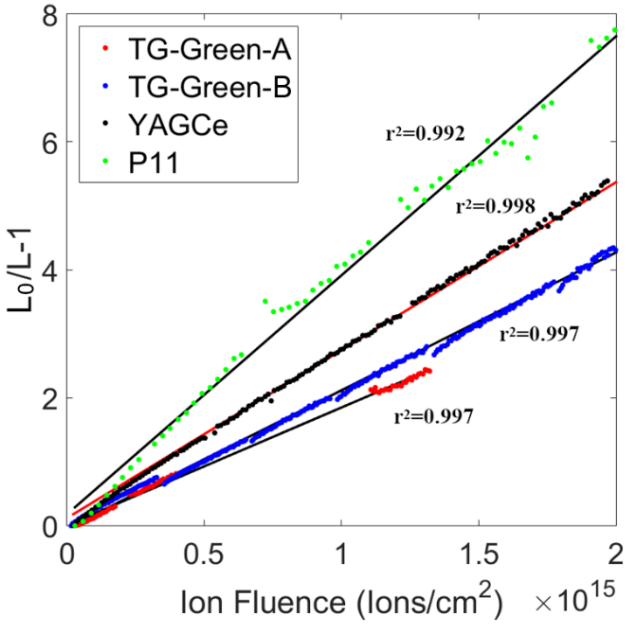

Figure 2. Black-Birk model fit of the scintillators: TG-Green-A (red), TG-Green-B (blue), YAGCe (black) and P11 (green, multiply by a factor 0.1).

previous work [13], suggest that heavy ion irradiation inhibits light emission faster than light ions in TG-Green and YAGCe scintillators. We speculate that this might be due to a larger fraction of the incident energy being transferred through nuclear collisions, and thus favouring the formation of defects, when irradiating with heavy ions as compared to light ions. However, this deserves a more in depth analysis which is out of the scope of this paper and left for future work.

Table 2. $F_{1/2}$ of the scintillators calculated using 2 different methods for 55 keV ion impact.

Scintillator	Black-Birk Model (10^{14} ions/cm^2)	Fluence at the emission value of 50% (10^{14} ions/cm^2)
TG-Green-A	5.4 ± 0.01	5.4 ± 0.1
TG-Green-B	4.64 ± 0.02	4.9 ± 0.1
YAGCe	3.81 ± 0.02	3.6 ± 0.1
P11	0.27 ± 0.01	0.69 ± 0.01

4.2 Calibrated photon detection yield of scintillators as a function of incident ion energy

The ionoluminescence efficiency or yield is expressed as the ratio between the number of emitted photons and incident ions [7, 8]. Figure 3 shows the scintillator efficiency as a function of incident $^{133}Cs^+$ ions energy. Two different scintillator positions were irradiated at TG-Green-A (TG-Green-A-I and TG-Green-A-II). For TG-Green-A-I and TG-Green-B measurements, a set of consecutive shots was done starting with a beam at 55 keV and then following the order: 5-10-20-30-40-50 keV and finally a repetition at 55 keV. Also, YAGCe measurements shots at 60, 65 and 70 keV were conducted. Only three measurements were performed on P11: 40, 50 and 60 keV. The investigated range of

2022 JINST 17 P02026

energies is the relevant one for the i-HIBP operation at ASDEX Upgrade, i.e. from 30–70 keV, which would correspond to plasma operation with magnetic fields on axis ranging from 1.5 to 2.5 T approximately [2].

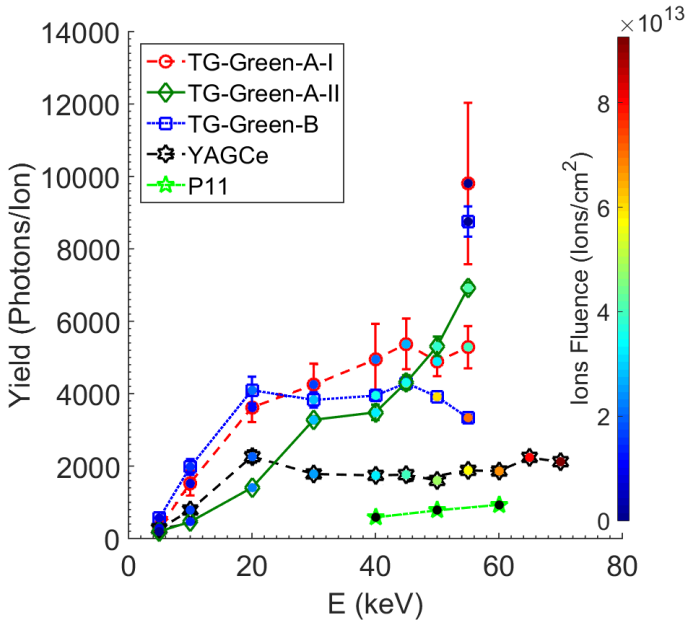

Figure 3. Ionoluminescence yield of the studied scintillators: TG-Green-A (red & dark green), TG-Green-B (blue), YAGCe (black) and P11 (green).

Two measurements of the incident number of ions were set by the Faraday Cup (see section 2). On the other hand, the number of emitted photons at certain energy is the mean value of a distribution integrated by SpectraSuit during the measurement. The yield errorbars are obtained by propagating the errors from the Faraday Cup measurements and the standard deviation of the number of photons distribution.

As we can see in figure 3, TG-Green-A and TG-Green-B have a very similar efficiency, followed by YAGCe and at last P11, which presents the lowest yield of the scintillators under study. The final measurement at 55 keV for TG-Green-A-I and TG-Green-B delivers a much lower yield than the first one. This indicates that the scintillator degradation during the shot sequence needs to be taken into account. This ionoluminescence degradation is a consequence of the ion fluencies the scintillators have received: $4 \cdot 10^{13}$ ions/cm^2 (TG-Green-A-I and TG-Green-A-II), $7 \cdot 10^{13}$ ions/cm^2 (TG-Green-B) and $9 \cdot 10^{13}$ ions/cm^2 (YAGCe) during the measurements. The three measurements at P11 were set at different scintillators position, where the fluence could be considered null. The efficiency of P11 increases linearly with energy. By looking at the lower energy points (5, 10 and 20 keV), where the fluence ($\sim 2 \cdot 10^{13}$ ions/cm^2) is still not high, the behaviour is also approximately linear for TG-Green-A, TG-Green-B and YAGCe. The linear behaviour at higher energies is weak, due to the degradation of the scintillators.

The yield dependence with incident energy has also been measured at the same scintillator position at which the degradation study was carried out (figure 4). We have irradiated the scintillators after this study until a decrease of the ionoluminescence with irradiation was not noticed anymore

2022 JINST 17 P02026

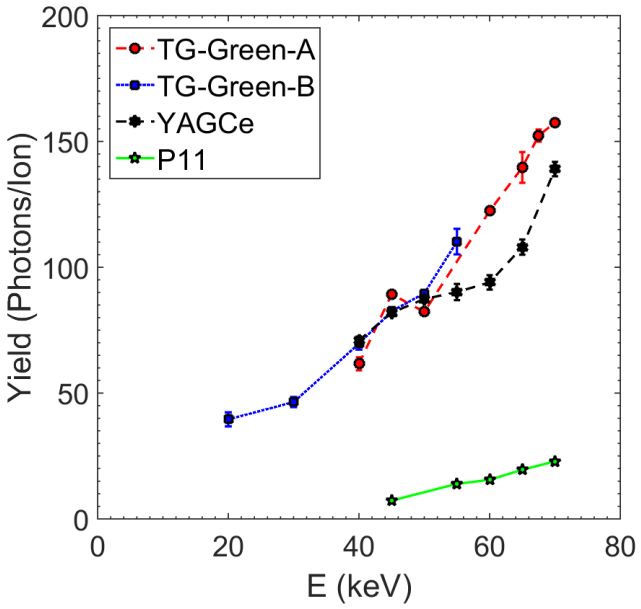

Figure 4. Scintillator yield as a function of incident ion energy in a degraded position of the scintillators (fluence > 1015 ions/cm^2): TG-Green-A (red), TG-Green-B (blue), YAGCe (black) and P11 (green).

(ion fluencies > 10^{15} ions/cm^2, see the following section). This is useful to know what signal levels we would expect at the i-HIBP once the scintillators are fully degraded. In these "fully-damaged" positions of the scintillators the yield is also observed to increase with the incident ion energy, but the calibrated photon detection yield is approximately 1% of a non-degraded one.

Table 3. Yield of the scintillators calculated using 2 different methods.

Scintillator	Yield Study (10^3 Photons/Ion)	Linearity Study (10^3 Photons/Ion)
TG-Green-A	8.8 ± 0.4	5.1 ± 0.8
TG-Green-B	9.8 ± 2.2	6.1 ± 1.1
YAGCe	1.9 ± 0.1	1.8 ± 0.5

4.3 Linearity of ionoluminiscence with ion current

A linear response of the scintillators ionoluminescence with incident ion current is required for the i-HIBP diagnostic. Due to its low efficiency, P11 was omitted from this study. To study this characteristic, we carried a sequence of shots using a beam energy of 55 keV and variable ion current. The latter was modified by changing the temperature of the ion source. During each of these sequences, we shot into the same spot of the scintillators. In figure 5 the results of several beam shots with an energy of 55 keV and variable intensity of ions are shown. In all cases a linear dependence of the scintillator yield was observed. The slope of the fit is the ionoluminescence yield of the scintillators at 55 keV. A comparison between the results of this linearity study with the yield study is set in table 3.

2022 JINST 17 P02026

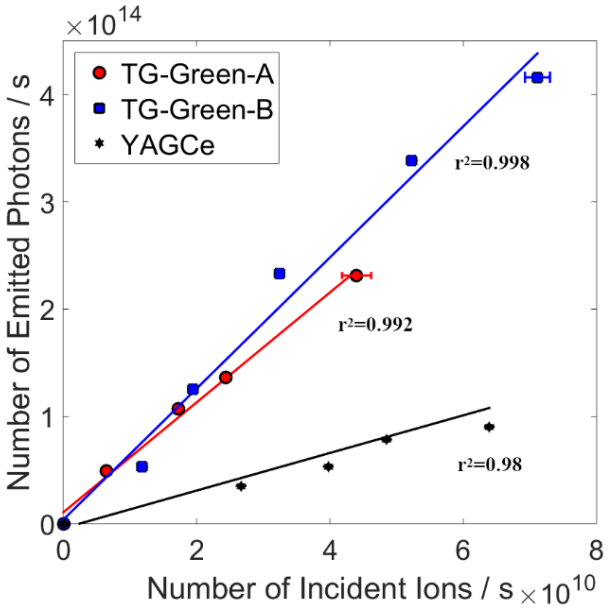

Figure 5. Linear behaviour of the scintillators with incident ion current at 55 keV: TG-Green-A (red), TG-Green-B (blue) and YAGCe (black).

4.4 Composition and thickness of the scintillators

The composition and thickness of the samples was studied by means of Ion Beam analytical techniques. The 3 MV Tandem accelerator of the Centro Nacional de Aceleradores (CNA) in Seville was employed to perform simultaneous RBS (Rutherford Backscattering Spectrometry) and PIXE (Particle Induced X-ray Emission) measurements using a 3 MeV proton beam with intensity ≈ 3 nA and 0.5 mm diameter. The electrically isolated target holder was biased to +300 V to prevent secondary electrons from escaping from the samples. For the RBS measurements a light-tight Si detector, placed at the scattering angle of 160°, was used to avoid receiving the ion-induced photons in the samples that would, otherwise, introduce noise into the spectra. We have assumed there are no concentration gradients in the scintillators materials in order to estimate their thickness. For PIXE analysis a LeGe (Low Energy Germanium) detector, placed at 145°, was used to have high efficiency up to 50 keV, in order to be able to detect the K-lines of the heavy elements present in the scintillator coatings (Ba, Eu), since their L-lines overlap with the K-lines of the substrate (Cr, Fe). In some measurements, a 250 µm thick mylar filter was placed in front of the LeGe detector to minimize pile-up events. The RBS and PIXE spectra were analysed using the SIMNRA [16] and GUPIX codes, respectively.

Figure 6 shows PIXE spectra of the TG-Green-A, TG-Green-B and YAGCe samples. In figure 6 (a), the presence of the dopant element (Eu) in samples TG-Green is clearly identified through its K-lines, but the concentration of Ce in the YAGCe film is below the detection limit (≈ 0.2% at). The RBS analysis (figure 7) also confirms that its Ce concentration must be ≤ 0.15%. On the other hand, while the stoichiometry of the YAGCe and TG-Green-B samples are close to their nominal values, the sample deposited in the CNA, apart from the expected elements (Sr, Eu), presents a huge amount of Ba, Si, O and N, which probably comes from the not yet optimized manufacturing method. The presence of these elements and the presence of Ga and S could explain

2022 JINST 17 P02026

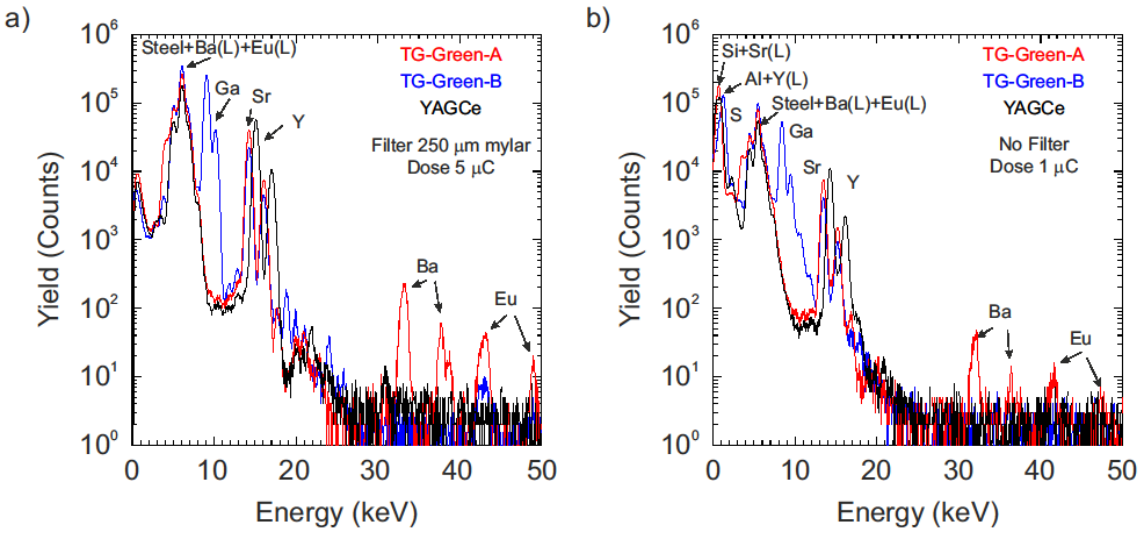

Figure 6. PIXE analysis of the materials: TG-Green-A (red), TG-Green-B (blue) and YAGCe (black) with (a) a mylar filter of 250 μm thickness and (b) without filter.

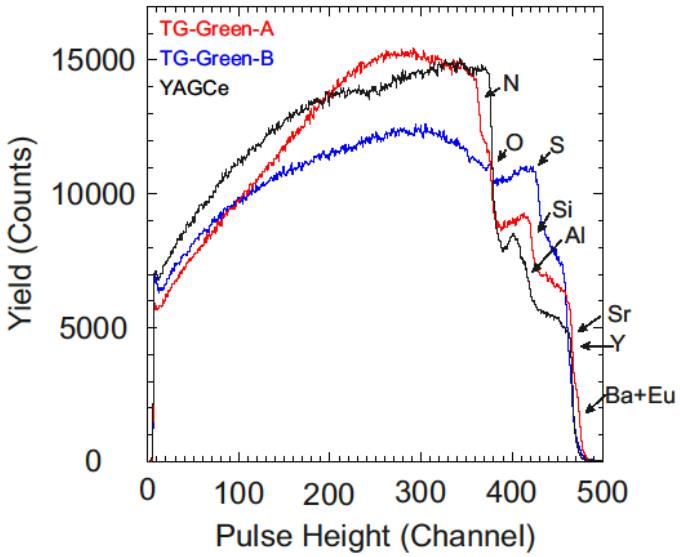

Figure 7. RBS analysis of the materials: TG-Green-A (red), TG-Green-B (blue) and YAGCe (black).

the difference between TG-Green-A and TG-Green-B light emission spectrum (see section 2). An Energy Dispersive X-Ray (EDX) Spectroscopy was made confirming the PIXE results. The physical thickness of TG-Green-A was too high to be measured by this method.

5 Summary and conclusions

The ionoluminescence of the scintillators (TG-Green-A, TG-Green-B, YAGCe and P11) by irradiating with ^{133}Cs beam has been characterized in order to use these materials as the active component of the new i-HIBP diagnostic at ASDEX Upgrade. In this work we have investigated the following

2022 JINST 17 P02026

Table 4. Results of PIXE and RBS analysis. a Supposing a density = 3.65 g/cm^3. b Supposing a density = 4.55 g/cm^3

Scintillator	Concentration (% at)	Thickness (10^{15} at/cm^2)	Physical thickness (µm)
TG-Green-A	Si(43) O(24) N(20) Sr(10) Ba(2) Eu(1)	75.000	-
TG-Green-B	Sr(11) Ga(26) S(62) Eu(1)	33.000	7.4^a
YAGCe	Y(13.1) Al(23.1) O(63.8)	100.000	10^b

ionoluminescence characteristics: the yield (number of photons emitted per incident ion), the degradation of the ionoluminescence and the linearity of emission with incident current. The main observations are:

- The highest yield is obtained for TG-Green-A. For an incident ion beam energy of 55 keV, it is close to 10^4 photons/ion.
- Strong degradation is observed for all studied scintillators at 55 keV ion energy irradiation. P11 shows the fastest degradation, with a $F_{1/2}$ of $2.7 \cdot 10^{13}$ ions/cm^2 and TG-Green-A the slowest, with a $F_{1/2}$ of $5.4 \cdot 10^{14}$ ions/cm^2. These measurements are added to previous results [14], filling the gap of irradiation with heavy ions in the low energy range (< 100 keV), and therefore may help to validate models of scintillator degradation. A more thorough investigation on this topic is out of the scope of this manuscript and is left for future work.
- All scintillators show a linear response with incident currents of the order of 10^{10} ions/s. Expected current densities at the i-HIBP scintillator plate are of the order of 1 mA/m^2 $\sim$ 10^{12} ions/(s·cm^2) in the i-HIBP diagnostic, which means $\sim 10^{10}$ ions/s using an incident beam of 1 mm of diameter.
- The low degradation, the high yield and the linearity of the light emission with incident current of YAGCe, TG-Green-A and TG-Green-B make these scintillators solid candidates to be used in i-HIBP diagnostic. Overall TG-Green is the better choice due to its higher yield and slower degradation.

On the other hand, previous works [8] have shown that high temperatures inhibit light emission as ion fluence does by creating defects on the scintillator. Although the temperature at the scintillator plate has been measured to be below 100°C during plasma operation, a high temperature resistance of the scintillator is still desired. Furthermore, due to the high-frequency of certain phenomena that will be studied by the i-HIBP diagnostic [1], a fast (< 1 µs) temporal response of the scintillator is needed. The temporal response of TG-Green has been characterized in previous work when irradiated by light ions [8], where it was found to be of the order of the range between 350 and 500 ns. The study of these properties of the TG-Green when irradiated by heavy ions will be the subject of future work.

As discussed in the previous paragraphs expected current densities at the i-HIBP scintillator plate are of the order of mA/m^2 $\sim$ 10^{12} ions/(s·cm^2) (this is an estimation since the signal levels are sensitive to plasma profiles [1]). This corresponds to a light yield of 10^{15} photons/s, associated purely to the irradiation due to the probe beam and considering a yield of the order of 10^3 photons/ion (see

2022 JINST 17 P02026

table 3). If we consider $F_{1/2}$ from table 2 for TG-Green A, we can estimate the plasma operation time needed to degrade the scintillator emission to this point. Assuming a shot length of 10 s, this leads to 86 shots before the ionoluminescence is reduced to 50%. From the point of view of data evaluation, a precise knowledge of the scintillator yield is needed to infer the plasma density profile and measure density fluctuations. Therefore, the fast degradation of the scintillator yield can be an issue. Possible solutions could be to keep track of the fluence at the scintillator plate using the current measurement available at the scintillator plate [1] and to perform regular cross-calibrations with other diagnostics capable of measuring the plasma density profile at the edge, such as the Li-BES available at AUG. However, this should not impact the capability of the diagnostic to measure plasma potential and magnetic field fluctuations, since these are inferred from the strike-line displacements.

Finally, although the scintillator screens investigated in this work are also sensitive to the irradiation by light ions, due to the geometry of the detector, no contamination of the i-HIBP signal is expected by these (e.g. fast-ions from external heating systems in the tokamak). This has been evaluated by numerical simulations performed with the FILDSIM code [17], and was confirmed during the 2021 campaign, were the i-HIBP was operated and no sign of light yield due to irradiation by fast-ions was observed.

Acknowledgments

This work received funding from the European Research Council (ERC) under the European Union's Horizon 2020 research and innovation programme (grant agreement No. 805162).

G. Birkenmeier acknowledges funding from the Helmholtz Association under grant no. VH-NG-1350. J. Galdon-Quiroga acknowledges funding from the Spanish Ministry of Science and Innovation under grant no. FJC2019-041092-I.

References

[1] G. Birkenmeier et al., *Beam modelling and hardware design of an imaging heavy ion beam probe for ASDEX Upgrade*, 2019 *JINST* **14** C10030.

[2] J. Galdon-Quiroga et al., *An imaging heavy ion beam probe diagnostic for the ASDEX Upgrade tokamak*, in proceedings of the *46th EPS Conference on Plasma Physics*, Milano, Italy, 8–2 July 2019, P1.1017.

[3] J. Galdon-Quiroga et al., *Conceptual design of a scintillator based imaging heavy ion beam probe for the ASDEX Upgrade tokamak*, 2017 *JINST* **12** C08023.

[4] J.B. Birks, *The Theory and Practice of Scintillation Counting*, Pergamon, New York (1964)

[5] M. García-Muñoz, H.-U. Fahrbach and H.Z. and, *Scintillator based detector for fast-ion losses induced by magnetohydrodynamic instabilities in the ASDEX upgrade tokamak*, *Rev. Sci. Instrum.* **80** (2009) 053503.

[6] M. García-Muñoz et al., *Characterization of scintillator screens for suprathermal ion detection in fusion devices*, 2011 *JINST* **6** P04002

[7] M. Jiménez-Ramos, J.G. López, M. García-Muñoz, M. Rodríguez-Ramos, M.C. Gázquez and B. Zurro, *Characterization of scintillator materials for fast-ion loss detectors in nuclear fusion reactors*, *Nucl. Instrum. Meth. B* **332** (2014) 216.

2022 JINST 17 P02026

[8] M. Rodríguez-Ramos, M. Jiménez-Ramos, M. García-Muñoz and J.G. López, *Temperature response of several scintillator materials to light ions*, *Nucl. Instrum. Meth. B* **403** (2017) 7.

[9] B. Zurro, C. Burgos, K.J. McCarthy and L.R. Barquero, *Design of luminescent detectors for the TJ-II device*, *Rev. Sci. Instrum.* **68** (1997) 680.

[10] S. Zoletnik, G. Anda, M. Aradi, O. Asztalos, S. Bató, A. Bencze et al., *Advanced neutral alkali beam diagnostics for applications in fusion research (invited)*, *Rev. Sci. Instrum.* **89** (2018) 10D107.

[11] SpectraSuite Spectrometer Operating Software, http://www.oceaninsight.com/.

[12] J.B. Birks and F.A. Black, *Deterioration of anthracene under α-particle irradiation*, *Proc. Phys. Soc. A* **64** (1951) 511.

[13] M. Rodriguez-Ramos, *Calibración absoluta y aplicación de los detectores de pérdidas de iones rápidos basados en materiales centelleadores para dispositivos de fusión nuclear*, Ph.D. Thesis, University of Seville (2017).

[14] C. Kim, W. Lee, A. Melis, A. Elmughrabi, K. Lee, C. Park et al., *A review of inorganic scintillation crystals for extreme environments*, *Crystals* **11** (2021) 669.

[15] R. Zhu, *Radiation damage in scintillating crystals*, *Nucl. Instrum. Meth. A* **413** (1998) 297.

[16] M. Mayer, *SIMNRA User's guide*, Tech. Rep., Report IPP 9/113, Max Planck Institute for Plasma Physics, Garching, Germany (1997).

[17] J. Galdon-Quiroga, M. Garcia-Munoz, M. Salewski, A.S. Jacobsen, L. Sanchis-Sanchez, M. Rodriguez-Ramos et al., *Velocity-space sensitivity and tomography of scintillator-based fast-ion loss detectors*, *Plasma Phys. Control. Fusion* **60** (2018) 105005.

2022 JINST 17 P02026